



## **Cohesion and Internal Friction of Fine Glass Beads as Affected by Small Intensity Vertical Vibration**

A. Castellanos, C. SoriaHoyo, J. M. Valverde, and M. A. S. Quintanilla

Citation: [AIP Conference Proceedings](#) **1145**, 707 (2009); doi: 10.1063/1.3180025

View online: <http://dx.doi.org/10.1063/1.3180025>

View Table of Contents: <http://scitation.aip.org/content/aip/proceeding/aipcp/1145?ver=pdfcov>

Published by the [AIP Publishing](#)

---

### **Articles you may be interested in**

[Applying 2D shape analysis techniques to granular materials with 3D particle geometries](#)

[AIP Conf. Proc.](#) **1145**, 833 (2009); 10.1063/1.3180057

[Dynamics of expanding holes in vertically vibrated wet granules](#)

[AIP Conf. Proc.](#) **1145**, 733 (2009); 10.1063/1.3180032

[Collapsing process of uniform granular slopes](#)

[AIP Conf. Proc.](#) **1145**, 601 (2009); 10.1063/1.3179998

[Compaction processes in granular beds composed of different particle sizes](#)

[J. Appl. Phys.](#) **98**, 123519 (2005); 10.1063/1.2149167

[Effects of vertical vibration on hopper flows of granular material](#)

[Phys. Fluids](#) **14**, 3439 (2002); 10.1063/1.1503354

---

# Cohesion and Internal Friction of Fine Glass Beads as Affected by Small Intensity Vertical Vibration

A. Castellanos, C. Soria-Hoyo, J. M. Valverde and M. A. S. Quintanilla

*Faculty of Physics. University of Seville. Avenida Reina Mercedes s/n, 41012 Seville. Spain.*

**Abstract.** We have used a novel centrifuge powder tester to obtain the angle of internal friction and cohesion of fine glass beads as affected by previous vibration in the vertical direction. In the experimental procedure we use a small amount of mass, typically between 2 and 4 grams, contained in a rectangular cell. The bed is initialized and subjected to low intensity vertical vibrations of controlled frequency and amplitude for a fixed period of time. By means of pre-vibration the material becomes compacted. Then the cell is taken to the centrifugal powder tester, in which it is rotated around its vertical axis at increasing values of the rotation velocity. At a critical point the shear stress caused by the action of the centrifugal force is large enough to drive material avalanches. From a theoretical analysis of these avalanches based on the Coulomb's method of wedges we derive the angle of internal friction and cohesion of the glass beads. Measurements have been performed using different masses pre-vibrated at different frequencies and amplitudes. Results from the tests are fitted to a single trend when they are plotted as a function of the effective consolidation stress imposed on the bed by means of pre-vibration. Basically, the data indicate a significant increase of cohesion and a slight decrease of the angle of internal friction as the effective consolidation on the sample is increased. The interparticle cohesion force has been estimated from the cohesion measured, and using the averaging Rumpf's equation. For the unconsolidated samples, the value estimated agrees with the expected force due to the sum of van der Waals and capillary forces for undeformed contacts between surface asperities. However, the interparticle cohesion force increases as pre-vibration intensity is increased, being this the main reason for the increase of cohesion at the bulk level. According to theoretical estimations, the increase of the interparticle cohesion force is attributable to the plastic yield of the surface asperities at contact. The rate of increase of the interparticle cohesion force with the interparticle consolidation force is in accordance with the results predicted by a theoretical model on plastic contacts between surface asperities. It can be concluded that fine powder flowability is seriously hindered by compaction due to pre-vibration.

**Keywords:** Cohesion, Granular flow, Vibration

**PACS:** 83.80.Fg, 81.20.Ev, 47.55.kf

Small intensity vertical vibration of a loosely packed bed induces compaction by helping grains to overcome arches and other barriers. Most of the processing plants dealing with fine powders experiment handling problems because of the lack of material flow predictability. While the large ratio of surface area to volume of fine powders provides high fluid-solid contact and reaction efficiencies, the relative strength of interparticle attractive forces is also increased, giving rise to poor flowability that is unpredictably affected by vibrations during powder transportation or storage when used is resumed. The Jenike shear cell [1] has been widely used to measure the angle of internal friction and cohesion of cohesive powders. Essentially the method consists of compacting a sample with a known external load into a cylindrical cell composed of two metal rings one upon the other. With the compaction load still applied the minimum steady state shear stress necessary to displace the upper ring horizontally with respect to the lower one is measured. According to the Mohr-Coulomb criterion, the angle of internal friction  $\varphi$  and the cohesion  $C$  of the powder are a measure of its capability to sustain shear stresses and therefore to flow [1]. Consider an arbitrary plane through the sample and a shear stress  $\tau$  acting on that plane; there

will be a critical value of the shear stress that will cause the material to shear off in that plane. This yield stress depend on the normal stress  $\sigma$  acting perpendicular to the plane. In his pioneer work, Coulomb approximated the relationship between  $\tau$  and  $\sigma$  by a linear function [1]

$$\tau = \sigma \tan \varphi + C \quad (1)$$

where  $C$  and  $\varphi$  are the cohesion and angle of internal friction of the granular material, respectively. Equation 1 defines the Mohr-Coulomb yield locus of the granular material. A problem of using the modified Jenike cell to investigate the flow properties of powders is that, in applications involving powder flow, the sample is usually in a state of small consolidation (typically in a range from a few Pa to a few hundred Pa), while in the Jenike shear cell the sample is initialized in a state of consolidations typically larger than 1 kPa. The Schulze ring shear tester [1] is a technical improve on the Jenike tester. This method is able to measure the yield locus at small consolidations and has been recognized as a standard technique for powder flow diagnosis. A general problem that besets shear testers is that, in order to relate the stresses to the real stresses inside the material, it must be assumed that the shear process takes place uniformly throughout

the sample [2], which is known to be false for overconsolidated materials [2]. In the case of highly cohesive powders, the shear occurs through fracture surfaces of uncertain location that are difficult to be erased by the initialization procedure used in the shear testers. In our experimental work we have estimated experimentally the angle of internal friction and cohesion of powder samples compacted by previous vertical vibration. Measurements have been carried out by means of a centrifuge powder tester (CPT) [3]. This device has been described in detail in ref. [4], in which results from measurements on diverse powders were also shown to illustrate its functioning.

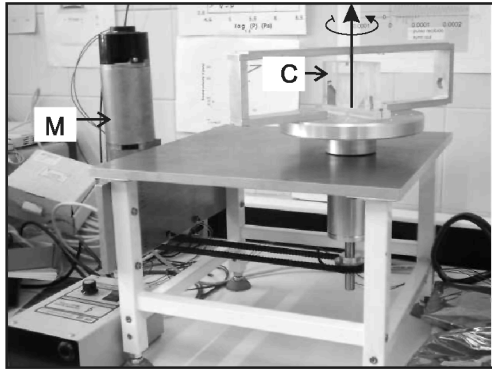


**FIGURE 1.** Photograph of the device built at the University of Seville to measure the angle of internal friction and cohesion of granular materials. The granular material rests on a rectangular cell (C) which is fixed to a rotatory plate. The motion is driven by a motor (M) which is controlled by a computer. A wireless camera (not shown) fixed to the rotatory structure records the evolution of the material as the cell is rotated.

In the experimental setup the sample of granular material partially fills a rectangularly shaped container of internal length  $2R = 8$  cm and 0.6 cm depth. The material is initialized by gently shaking the container horizontally to smooth the sample free surface and make it horizontal. After initialization, the container is mounted on an electromagnetic vibration exciter driven by a signal generator, which provides sinusoidal, vertical vibrations of controlled frequency  $\nu$  and amplitude  $A$ . During the pre-vibration procedure the sample is subjected to vertical oscillations at fixed amplitude and frequency for a time period of two minutes. Experiments have been performed at two selected frequencies (200Hz and 1kHz), which are controlled to within  $\pm 0.1$  Hz. We have tested soda-lime glass beads of diameter  $d_p \approx 40 \pm 10 \mu\text{m}$  and particle density  $\rho_p \approx 2500 \text{ kg/m}^3$ . The sample masses used to run the experiment are between 2 and 4 grams, corresponding to typical volumes between  $1.5 \text{ cm}^3$  and  $3 \text{ cm}^3$ . The height  $H$  of the material layer in the container is between 3 and 5 mm. The dimensionless peak acceleration amplitude  $\Gamma = A(2\pi\nu)^2/g_0$ , where  $g_0 = 9.81 \text{ m/s}^2$  is the acceleration due gravity, is in a range that extends

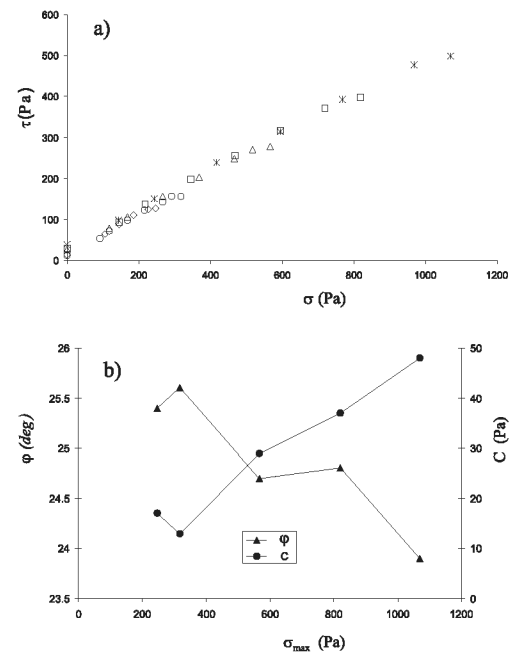


**FIGURE 2.** a) Yield loci measured for the fine glass beads and for different values of the maximum normal stress applied by a lid using the standard Schulze ring shear tester. b) Angle of internal friction (left axis) and cohesion (right axis) derived as a function of the maximum normal stress. The typical indeterminacy in the measurement of  $\phi$  is around  $1^\circ$  and it is around 10 Pa in the measurement of  $C$ .

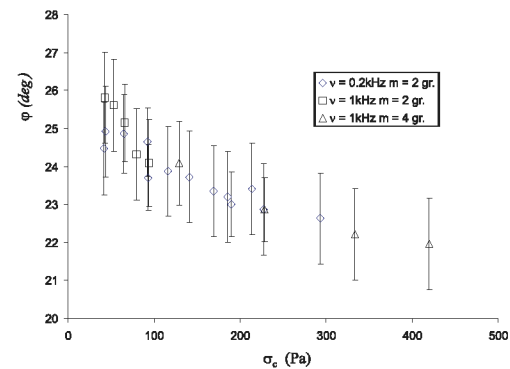


**FIGURE 3.** Experimental values of the angle of internal friction  $\phi$  for pre-vibrated samples as a function of the effective consolidation  $\sigma_c$  due to previous vibration. The inset indicates the frequency  $\nu$  of pre-vibration and the mass  $m$  of powder used.

up to  $\Gamma \approx 5$ , and can be controlled to within  $\pm 0.1g_0$ . When ramping up the vibration intensity we observe irreversible compaction of the powder layer that remains all the time attached to the base of the container. Thus, the net effect of vibration within the applied range of intensities is to increase the rms acceleration on the sample by a factor  $(1 + \Gamma)$ . The consolidation stress  $\sigma_{c,0}$  of

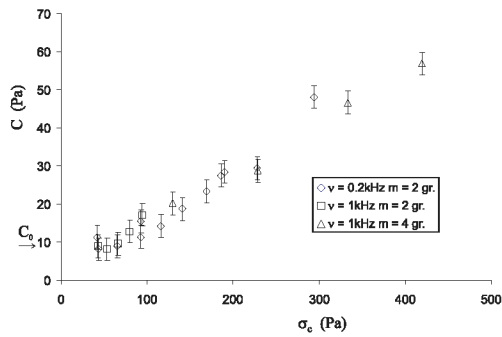


**FIGURE 4.** Average experimental values of cohesion  $C$  for pre-vibrated samples as a function of the effective consolidation stress  $\sigma_c$ , which is increased by previous vibration. The inset indicates the frequency  $\nu$  of pre-vibration and the mass  $m$  of powder used. The arrow in the vertical axis indicates the cohesion  $C_0 \simeq 10$  Pa measured for the nonvibrated samples, subjected to a consolidation stress just due to their own weight  $\sigma_{c0} \simeq 40$  Pa.

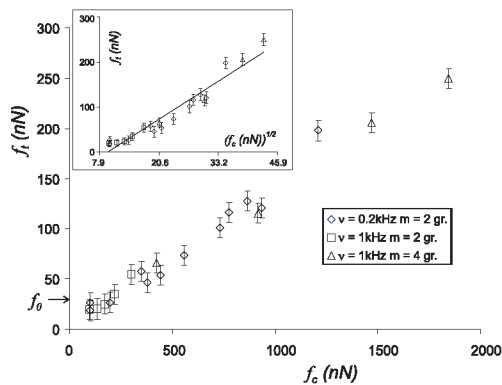


**FIGURE 5.** Estimated interparticle cohesion force as a function of the estimated interparticle consolidation force caused by previous vibration. The arrow in the ordinate axis indicates the interparticle force calculated by summation of the van der Waals and capillary forces. The inset is a plot of the interparticle cohesion force as a function of the square root of the interparticle consolidation force. The straight line is a linear fit to the data ( $R^2 = 0.938$ )

the nonvibrated sample, which is only due to its own weight, is small (typically  $\sigma_{c0} \simeq \rho_p \phi g_0 H \simeq 40$  Pa). By means of pre-vibration, the effective consolidation stress  $\sigma_c \simeq \sigma_{c0}(1 + \Gamma)$  is thus increased in a range extending up to  $\sigma_c \simeq 400$  Pa. Once the powder is compacted by vibrations it is carefully taken to the centrifuge powder tester (CPT). In Fig. 1 we show a photograph of the CPT built at the University of Seville. The container is placed on a rotatory table and it is rotated around its vertical axis. The rotation velocity is driven by a D.C. permanent magnet motor controlled by a computer. In the experiments reported in this paper the rotation velocity was steadily increased at a rate of 1rpm/s up to a maximum value

of 600rpm. At a critical point the shear stress caused by the action of a centrifugal force is large enough to drive material avalanches. The succession of avalanches are recorded by a wireless TV cam solidary to the container and later analyzed with the help of an image software to obtain the mechanical properties of the material as a function of pre-vibration intensity.

In order to compare our results with results from independent experiments we have tested the powder by using the Schulze ring shear tester (model RST-01.pc Computer-controlled). Figure 2 shows the yield loci measured for different values of the maximum normal stress  $\sigma_{max}$  initially applied by the lid on the powder. From this figure it can be concluded that the behavior of the powder can be well described by the Coulomb yield condition (Eq. 1), with an angle of internal friction  $\phi$  around  $25^\circ$  that decreases slightly as  $\sigma_{max}$  is decreased (see Fig. 2b). In Fig. 2b we have plotted also the cohesion calculated from the yield loci as a function of  $\sigma_{max}$ . It is seen that the cohesion increases as the maximum normal stress is increased. Measurements for  $\sigma_{max}$  below 200 Pa were not possible with sufficient accuracy.

Following the methodology described in detail in ref. [4] we obtain the experimental values of the angle of internal friction  $\phi$  from the measurement of the angle of the slope at high rotation velocities. Results show that within the experimental scatter the values of  $\phi$  do not depend on the rotation velocity employed for the calculation as should be expected. From these results it can be also inferred that the average angle of internal friction  $\langle \phi \rangle$  decreases slightly as pre-vibration intensity is increased. This correlation is seen in Fig. 3 where we have plotted  $\langle \phi \rangle$  as a function of the effective consolidation  $\sigma_c \simeq \sigma_{c0}(1 + \Gamma)$ . It is observed that  $\langle \phi \rangle$  decreases from about  $25^\circ$  at low consolidations to about  $22^\circ$  at the highest consolidations, although the experimental indeterminacy precludes us from a statistically significant conclusion. Nevertheless, note that the value of the angle of internal friction estimated for the non-vibrated sample (around  $25^\circ$ ) agrees with the average angle of internal friction derived from the yield loci measured using the ring shear tester (Fig. 2b). Moreover, the result obtained from the ring shear tester also indicates a decrease of  $\langle \phi \rangle$  as the maximum normal stress used to obtain the yield locus is increased. We can not establish however a direct comparison between both sets of data since the effective consolidation stress defined in our experiment is not directly related to the maximum normal stress applied by the lid on the powder using the ring shear tester. In Fig. 4 we have plotted the experimental values of cohesion  $C$  obtained from the measurement of the rotation velocity at which the first avalanche is observed. It is seen that cohesion increases as the effective consolidation is increased due to pre-vibration. This trend agrees with the tendency of observed using the ring shear tester

(Fig. 2b), albeit our apparatus is able to measure cohesion accurately in the range of smaller consolidations.

Using the Rumpf averaging equation [5], the interparticle cohesion force  $f_i$  can be estimated as  $f_i \sim \sigma_t \pi d_p^2 / \zeta \phi$ , where  $\sigma_t$  (tensile strength) is the maximum tensile stress that the powder can withstand and  $\zeta$  is the coordination number (average number of contacts per particle). The coordination number  $\zeta$  can be related to the particle volume fraction  $\phi$  by the equation  $\zeta \simeq (\pi/2)(1 - \phi)^{-3/2}$  (ref. [5]). Experimental tests on fine powders using a ring shear tester and a tilted fluidized bed technique [5] have shown that the yield locus of cohesive powders has a convex shape at very small and negative values of  $\sigma$ . As a first approximation, we will consider that the tensile strength  $\sigma_t$  and the cohesion  $C$  are of the same order of magnitude ( $C \sim \sigma_t$ ). Likewise the average consolidation force  $f_c$  transmitted to the interparticle contacts by the effective consolidation stress  $\sigma_c$  can be estimated. Estimations of the cohesive force between particles  $f_i$  as a function of the interparticle consolidation force  $f_c$  are plotted in Fig. 5. The data shows that, in the range of forces tested,  $f_i$  increases with  $f_c$  in about one order of magnitude, indicating that the increase of cohesion  $C$  at the bulk level is mainly attributable to the increase of the cohesive force at the micro-level of interparticle contacts.

For dry particles the interparticle attractive force arises mainly from van der Waals and capillary interaction. The van der Waals attractive force can be approximated by [5]  $f_{vdW} \simeq Ad^*/12z_0^2$ , where  $A$  is the Hamaker constant ( $A \simeq 1.5 \times 10^{-19}$  J for glass [5]),  $d^* = d_1 d_2 / (d_1 + d_2)$  is the reduced particle diameter, and  $z_0 \simeq 3 - 4 \text{ \AA}$  is the distance of closest approach between two molecules. Because of the short range of the molecular interaction, the van der Waals force is actually determined by the typical size of the surface asperities  $d_a$  instead of the particle diameters. A typical value reported for the size of surface asperities of fine powder particles is  $d_a \simeq 0.2 \mu\text{m}$ , which agrees with the average asperity diameter derived from AFM analysis of the surface of glass beads [5]. Thus we can estimate  $f_{vdW} \sim 10 \text{ nN}$  for our experimental particles.

The experiments are carried out at ambient conditions and it is therefore possible that moisture condensation at the asperities at contact yield attractive capillary forces. The capillary force between two equal spheres of radius  $r$  can be approximated by  $f_{cl} \simeq \pi \gamma r^2 \beta / S$ , where  $\gamma$  is the liquid surface tension,  $\beta$  is the half-filling angle and  $S$  is the separation distance [6]. For small water bridges  $S \simeq r\beta$ , we can write  $f_{cl} \simeq \pi \gamma r$  where  $r \sim d_a/2 \simeq 0.1 \mu\text{m}$  and  $\gamma = 72.75 \text{ mN/m}$ . Accordingly, the contribution to adhesion by the capillary force is  $f_{cl} \simeq 20 \text{ nN}$ . The total attractive force expected would be  $f_0 = f_{vdW} + f_{cl} \simeq 30 \text{ nN}$ , in agreement with the cohesive interparticle force es-

timated from our measurements for the loosely packed samples (see Fig. 5). Even small consolidation stresses may induce plastic deformation of the surface asperities at contact, thus enhancing the interparticle cohesive force [5]. The critical load on the contact  $P_Y$  for the initiation of plastic yield within the bulk of the particle can be calculated as  $P_Y \simeq 2\pi^3 (d_a^*)^2 Y^3 / 3E^2$ , where  $Y$  is the compressive yield strength,  $E$  is the Young modulus, and  $d_a^*$  is the reduced asperity diameter. For contacts between asperities of same size  $d_a^* = d_a/2$ . Using as typical values  $Y = 1100 \text{ MPa}$  (reported for glass [5]) and  $E = 68.9 \text{ GPa}$  (reported for soda-lime glass [5]), it is estimated  $P_Y \simeq 20 \text{ nN}$ , which is lower than the smallest consolidation forces that we estimate in our experiments (see Fig. 5). Mesarovic and Johnson [5] have proposed the relationship

$$f_i \simeq \frac{3\sqrt{\pi}}{2} \frac{wE^*}{H^{3/2}} \sqrt{f_c} \quad (2)$$

where  $1/E^* = 2(1 - \nu^2)/E$ , being  $\nu$  the Poisson ratio ( $\nu = 0.16$  for soda-lime glass [5]),  $w = 2\gamma$  is the work of adhesion, being  $\gamma$  the surface energy of the solid ( $\gamma \simeq 0.3 \text{ J/m}^2$  for glass [5]), and  $H \approx 3Y$  is the hardness of the solid material. The best linear fit to data of  $f_i$  vs.  $\sqrt{f_c}$  (see inset of Fig. 5) yields a slope of  $6.65 \text{ (nN)}^{1/2}$ , which agrees in order of magnitude with the values predicted by Eq. 2 (the calculated slope is  $9.41 \text{ (nN)}^{1/2}$ ) using  $w = 0.6 \text{ J/m}^2$ ,  $E = 68.9 \text{ GPa}$ ,  $\nu = 0.16$  and  $H = 3300 \text{ MPa}$ .

## ACKNOWLEDGMENTS

We acknowledge Spanish Government Agency Ministerio de Ciencia y Tecnologia (contract FIS2006-03645) and Junta de Andalucia (contract FQM 421).

## REFERENCES

1. Schwedes J. *Granular Matter* 2003;1:43.
2. Svarovsky L. Powder Testing Guide: Methods of Measuring the Physical Properties of Bulk Powders. Elsevier Applied Science, England (1987).
3. Castellanos A, Quintanilla MAS, Valverde JM. Patent no. WO 2007/042585 A3 (University of Seville). April 19, 2007.
4. Castellanos A, Quintanilla MAS, Valverde JM, Soria-Hoyo C. *Rev. Sci. Instrum.* 2007;78:073901(1-10).
5. Castellanos A. *Adv. Phys.* 2005;54:263-376.
6. Willett CD, Adams MJ, Johnson SA, Seville JPK. *Langmuir* 2000;16:9396-9405.